COMMUNICATION

CaO-based sorbents for CO$_2$ capture prepared by ultrasonic spray pyrolysis†

Maryam Sayyah,‡[b] Brandon R. Ito,‡[a] Massoud Rostam-Abadi,[c] Yongqi Lu[c] and Kenneth S. Suslick*[a]

We report the ultrasonic spray pyrolysis (USP) synthesis and characterization of composite calcium oxide-based sorbents for carbon dioxide capture. Inclusion of a small amount of Al$_2$O$_3$ into the CaO matrix (as low as Al/Ca: 0.03) yielded significant enhancement of resistance to recycling degradation. The effective homogenous dispersion of additives in the CaO matrix and the relatively high surface area materials obtained *via* USP explain the sorbent's high performance. All materials were characterized by XRD, STEM, TEM, SEM, and TGA (for CO$_2$ uptake measurements). Two common phases of CaAl$_x$O$_y$, Ca$_{12}$Al$_{14}$O$_{33}$ and Ca$_3$Al$_2$O$_6$, were formed during multiple cycles of calcination and CO$_2$ uptake.

Carbon dioxide sequestration has become a subject of extreme interest in recent years as a path towards greenhouse gas mitigation. The combustion of fossil fuels for power generation accounts for over one third of anthropogenic carbon dioxide emission sources, so substantial research has focused on CO$_2$ capture and sequestration from such sources.[1] Many materials are currently under investigation for CO$_2$ capture, both for post-combustion (*e.g.*, silica supported amines,[2] zeolites,[3] activated carbons[4]) and for "pre-combustion", *i.e.*, after water–gas shift (WGS) but before power generation (*e.g.*, CaO,[5] lithium zirconates,[6] hydrotalcites,[7] and metal–organic frameworks[8]). Sorbents that operate at relatively high temperature (*i.e.* CaO) are particularly attractive choices for pre-combustion scheme to integrate with WGS or methane steam reforming processes.[9] A

sorption-enhanced water–gas shift reaction process (SEWGS) combines the WGS reaction and CO$_2$ removal into a single process step in an integrated gasification combined cycle (IGCC) power plant.[1,9] In SEWGS, a solid sorbent is employed to capture the CO$_2$ generated by the WGS reaction. A key technical issue for the SEWGS is to identify and develop sorbents that can capture CO$_2$ under high pressure and high temperature syngas conditions and minimize or even eliminate the need for WGS catalysts.

Calcium oxide has emerged as an attractive material for high temperature CO$_2$ capture because it is inexpensive, has high selectivity, and rapid kinetics. CaO, however, suffers from rapid degradation of capacity after multiple carbonation/calcination cycles due to reduction of surface area.[10] The decline in the performance of CaO materials during cycling are generally attributed to loss of microporosity[11] and sintering.[12]

Several approaches have been taken to improve the performance of CaO over multiple cycles, including the addition of supports and binders such as carbon,[13] magnesium oxide,[14] and calcium aluminates.[15] Some researchers have modified the sorbent microstructure to improve the sorbent stability.[16] Additionally, it has been shown that the sorbent can be partially regenerated upon hydration.[17]

Aerosol synthesis methods have been extensively utilized to prepare a variety of metal oxides, even on an industrial scale.[18,19] We report here the first use of ultrasonic spray pyrolysis (USP) as a continuous flow method for the facile synthesis of CaO-based materials for CO$_2$ capture applications. In order to improve cyclic reversibility of the prepared sorbents, Al$_2$O$_3$ was incorporated into CaO matrix. It has been previously noted that Al$_2$O$_3$ forms mixed calcium aluminate phases upon reaction with CaO at high temperatures (*e.g.* Ca$_{12}$Al$_{14}$O$_{33}$, Ca$_3$Al$_2$O$_6$, CaAl$_2$O$_4$).[15b] To synthesize the composite aluminum-doped CaO materials, a solution of calcium nitrate tetrahydrate [Ca(NO$_3$)$_2$·4H$_2$O] and aluminum nitrate nonahydrate [Al(NO$_3$)$_3$·9H$_2$O] in ethanol were nebulized *via* ultrasound, and the resulting mist was carried through a furnace tube (set at 600 °C unless otherwise stated) by argon gas. Solvent evaporation and precursor

[a]*Department of Chemistry, School of Chemical Sciences, University of Illinois at Urbana-Champaign, 600 S. Mathews Ave., Urbana, IL 61801, USA. E-mail: ksuslick@illinois.edu; Fax: +1 217 244 318; Tel: +1 217 333 2794*

[b]*Department of Chemical and Biomolecular Engineering, School of Chemical Sciences, University of Illinois at Urbana-Champaign, 600 S. Mathews Ave., Urbana, IL 61801, USA. E-mail: msayyah2@illinois.edu; Tel: +1 217 333 1532*

[c]*Illinois State Geological Survey, Prairie Research Institute, University of Illinois at Urbana-Champaign, 615 E. Peabody Dr., Champaign, IL 61820, USA*

† Electronic supplementary information (ESI) available: A schematic of the USP-setup and additional materials characterization. See DOI: 10.1039/c3ra44566f

‡ These authors contributed equally.

decomposition occurred within the furnace, and the product was collected in ethanol-filled bubblers. A schematic of the USP set-up is presented in the ESI (Fig. S1†). The nitrate salts were selected as precursors for two reasons: first, each salt decomposes completely to the respective oxide leaving no residue behind; and second, the gases created during nitrate decomposition act as porogens and increase the surface area of the sorbent product. Several studies have shown that the performance of CaO sorbents is directly related to the surface area of the material.[11,12]

Sorbents containing various ratios of Al/Ca were synthesized by USP. XRD of the as-synthesized materials show only crystalline $CaCO_3$ (Fig. 1a). The Debye–Sherrer formula was used to calculate the $CaCO_3$ crystallite size based on the six major characteristic peaks of $CaCO_3$ pattern (ICDD PDF card 04-007-8659) at 23.05, 29.4, 35.9, 39.4, 43.1 and 48.5°. $CaCO_3$ crystallite size comparison between pure $CaCO_3$ and Al/Ca materials with an atomic ratio of 0.16 reveals that the presence of Al reduced the grain size from 133 nm to 45 nm, which suggests that the alumina phase exists as an amorphous phase between $CaCO_3$ grains. USP produces the carbonated form of CaO ($CaCO_3$) due to reaction with CO_2 produced from the pyrolysis of the solvent, ethanol. In order to confirm formation of a CaAlO phase, a sample with Al/Ca = 0.16 was calcined at 900 °C for 1.5 h; from the XRD pattern (Fig. 1b) small peaks corresponding to mayenite ($Ca_{12}Al_{14}O_{33}$) phase were observed. As described in

more detail later, the sorbents subjected to 15 cycles of calcination/carbonation; XRD characterization of the cycled sample reveals the formation of both $Ca_{12}Al_{14}O_{33}$ and $Ca_3Al_2O_6$ phases (Fig. 1c). This indicates that intermediate mayenite phase observed in Fig. 1b turns into the more stable $Ca_3Al_2O_6$ phase after increased cycles of calcination/carbonation. As expected, increasing the amount of Al in the synthesis produces more pronounced CaAlO peaks.

This specific Al/Ca ratio (0.16) was chosen as a representative sample for characterization purposes for several reasons. First, this composition has been previously studied heavily in the literature,[15] so it is a good choice for comparison. Second, a sample with Al/Ca = 0.16 corresponds to a composition of 75 : 25 wt% CaO : $Ca_{12}Al_{14}O_{33}$ after full transformation to the calcium aluminate phase; 75 : 25 is obviously arbitrary, but certainly representative. Third, lower ratios of Al/Ca make the XRD identification of the aluminate phase difficult due to the low intensity of the calcium aluminate peaks.

STEM-EDX analysis was done on a particle with Al/Ca = 0.16 as shown in Fig. 2. The particles are macroporous with a homogenous distribution of Al and Ca throughout, as seen in Fig. 2b and c. The ratio of maximum counts of Ca and Al K_α signals is ~0.17 which is consistent with the atomic ratio for the sample composition (Al/Ca = 0.16). TEM images for various sorbent compositions (Fig. S2†) reveal the change in particles' morphology from hollow to solid structure upon increasing alumina content in the sorbents. Pure $CaCO_3$ particles are mostly hollow spheres (Fig. S2a†), and increasing the Al/Ca ratio tends to make a solid macroporous morphology. N_2 BET surface analysis (Table S1†) shows that the surface areas of each sorbent is ~25 m^2 g^{-1}.

As a control, the effect of synthesis temperature on the sorbent's stability for the pure CaO sorbents was investigated. As shown in Fig. S5†, the synthesis temperature does not have much influence on the cycling stability of the materials nor does it change the morphology. Also, as indicated throughout the literature,[11] regeneration conditions (temperature and CO_2 concentration) have a stronger influence on the stability of the CaO sorbents than preparation parameters. Therefore, we chose the lowest synthesis temperature for which we obtained the complete decomposition of nitrate precursor to oxide (i.e., 600 °C).

Then CO_2 uptake of composite CaO-based sorbents was compared for various sorbent compositions during 15 cycles of calcination/carbonation (Fig. 3). Initial CO_2 uptake decreases
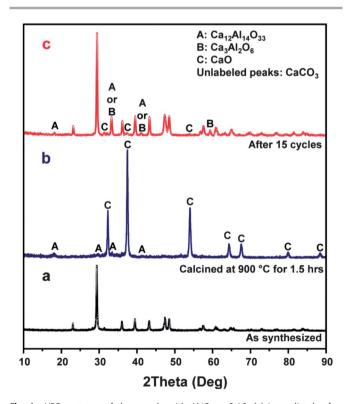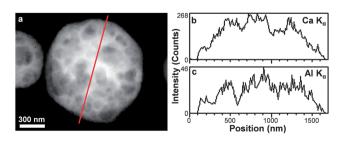

Fig. 1 XRD patterns of the sample with Al/Ca = 0.16; (a) immediately after collection from the USP setup, (b) after calcination at 900 °C for 1.5 h and (c) after 15 cycles of calcination/carbonation. The XRD peak labels given for $CaCO_3$, $Ca_{12}Al_{14}O_{33}$, $Ca_3Al_2O_6$ and CaO are from ICDD PDF cards 04-007-8659, 00-009-0413, 04-008-8069 and 04-005-4757 respectively.

Fig. 2 (a) STEM image and EDX line scan analysis of a particle with Al/Ca 0.16; (b) Ca K_α signal with 268 max counts, and (c) Al K_α signal with 46 max counts. The red line in (a) indicates the line scan analysis path (~1.7 μm, 15 analysis points).
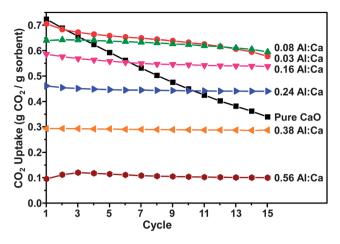
Fig. 3 CO_2 uptake by Al-containing sorbents during 15 cycles of calcination/carbonation; calcination at 950 °C for 5 min under 100% N_2 and carbonation at 710 °C for 30 min under 100% CO_2. Incorporating low concentrations of Al_2O_3 significantly improves the cycling stability over 15 cycles.

Fig. 5 SEM images of the hollow pure CaO sorbent. (a) After 2 cycles of calcination/carbonation. (b) After 25 cycles of calcination/carbonation. This picture shows that CaO particles retained their spherical morphology after a few cycles of adsorption/desorption and lost their structure in an increased number of cycles.

from the addition of inert Al_2O_3, whereas the recycling stability showed a significant improvement even with low concentrations of Al_2O_3 present (e.g., as low as 0.03 Al to Ca ratio). Carbonation and calcination cycles were performed at 710 °C for 30 min under 100% CO_2 and 950 °C for 5 min under 100% N_2, respectively (see ESI† for more details on the TGA protocol). A comparison of the performance of Al/Ca = 0.16 sorbent developed in this work with others of its kind is shown in the Table S2†. The performance of the USP samples is improved compared to prior literature. More importantly, USP is a scalable flow process that produces small particles with high surface areas and relatively uniform particle size. Prior methods of synthesis are batch, do not yield small particle size, and often do not give uniform distribution of Al.

SEM and TEM images of the sorbent with Al/Ca = 0.16 show that the morphology consists of isolated microspheres (~2 μm diameter) before cycling (Fig. 4a and S2d†). During cycling, progressively larger agglomerates are formed (>200 μm, as shown in Fig. S3b and c†). Higher magnification images of the surface of the agglomerates (Fig. 4b and c) reveal, however, that the spherical microstructure of the particles are still intact, although less so after 15 cycles.

One of the reasons that we embarked on this study was to test the stability of hollow CaO spheres with respect to repeated carbonation and calcination. The molar volume change from

CaO to $CaCO_3$ is very large (i.e., an increase of ~120% in the molar volume) and this generally causes fracture of solid CaO particles with the consequent formation of fines. We had initially hypothesized that hollow microspheres of CaO might better retain their morphology: the spherical shape is structurally much stronger than a solid microparticle and in addition the internal hollow might permit the molar expansion upon CO_2 uptake to occur without fragmentation. USP provides a particularly easy method to create hollow microspheres,[18–20] and we are able to easily produce hollow $CaCO_3$ microspheres by USP of solutions of $Ca(NO_3)_2$ in ethanol (Fig. S2a†). From SEM characterization, we do indeed observe that after two cycles of carbonation/calcination, the microsphere structure is retained (Fig. 5a). After further cycling (>15 cycles), however, the solid CaO sinters significantly, in spite of retention of the microsphere morphology (Fig. 5b). The hollow microspheres of pure CaO thus did not prove to be stable to cycling of carbonation/calcination.

Conclusions

In summary, we have synthesized a series of macroporous $CaAl_xO_y$ materials for CO_2 capture via ultrasonic spray pyrolysis. USP provides a facile and scalable route for materials synthesis.[19] The formation of calcium aluminate phases greatly stabilizes the CO_2 capacity of the sorbent over 15 calcination/carbonation cycles and provides a more stable sorbent than traditional batch preparations. Over 15 cycles, the optimum Al/Ca ratio is about 0.08.
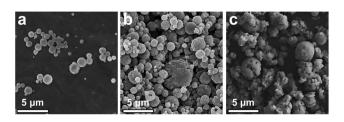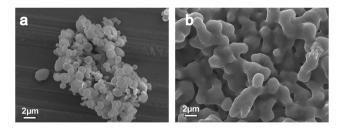
Acknowledgements

Fig. 4 High magnification SEM images of the sorbent with Al/Ca = 0.16. (a) before cycling (b) after 2 cycles of calcination/carbonation. (c) after 15 cycles of calcination/carbonation.

References

1 S. Choi, J. H. Drese and C. W. Jones, *ChemSusChem*, 2009, **2**, 796–854.

2 A. Sayari and Y. J. Belmabkhout, *J. Am. Chem. Soc.*, 2010, **132**, 6312–6314.

3 A. Zukal, I. Dominguez, J. Mayerová and J. Cejka, *Langmuir*, 2009, **25**, 10314–10321.

4 (*a*) T. C. Drage, J. M. Blackman, C. Pevida and C. E. Snape, *Energy Fuels*, 2009, **23**, 2790–2796; (*b*) G. P. Hao, W. C. Li, D. Qian and A. H. Lu, *Adv. Mater.*, 2010, **22**, 853–857.

5 H. Gupta and L. S. Fan, *Ind. Eng. Chem. Res.*, 2002, **41**, 4035–4042.

6 A. Iwan, H. Stephenson, W. Ketchie and A. Lapkin, *Chem. Eng. J.*, 2009, **146**, 249–258.

7 M. K. R. Reddy, Z. P. Xu, G. Q. Lu and J. C. D. da Costa, *Ind. Eng. Chem. Res.*, 2006, **45**, 7504–7509.

8 A. R. Millward and O. M. Yaghi, *J. Am. Chem. Soc.*, 2005, **127**, 17998–17999.

9 (*a*) R. W. Breault, *Energies*, 2010, **3**, 216–240; (*b*) A. Lopez Ortiz and D. P. Harrison, *Ind. Eng. Chem. Res.*, 2001, **40**, 5102–5109; (*c*) C. Wu and P. T. Williams, *Fuel*, 2010, **89**, 1435–1441.

10 (*a*) R. Barker, *J. Appl. Chem. Biotechnol.*, 2007, **23**, 733–742; (*b*) R. Barker, *J. Appl. Chem. Biotechnol.*, 1974, 221–227; (*c*) G. Grasa, B. González, M. Alonso and J. C. Abanades, *Energy Fuels*, 2007, **21**, 3560–3562.

11 (*a*) J. Abanades, *Chem. Eng. J.*, 2002, **90**, 303–306; (*b*) J. C. Abanades and D. Alvarez, *Energy Fuels*, 2003, **17**, 308–315.

12 (*a*) V. Manovic and E. J. Anthony, *Energy Fuels*, 2010, **24**, 5790–5796; (*b*) P. Sun, J. R. Grace, C. J. Lim and E. J. Anthony, *AIChE J.*, 2007, **53**, 2432; (*c*) J. Wang and E. J. Anthony, *Ind. Eng. Chem. Res.*, 2005, **44**, 627–629.

13 Z. Wu, N. Hao, G. Xiao, L. Liu, P. Webley and D. Zhao, *Phys. Chem. Chem. Phys.*, 2011, **13**, 2495–2503.

14 (*a*) M. Bhagiyalakshmi, J. Y. Lee and H. T. Jang, *Int. J. Greenhouse Gas Control*, 2010, **4**, 51–56; (*b*) M. Sayyah, Y. Lu, R. I. Masel and K. S. Suslick, *ChemSusChem*, 2013, **6**, 193–198.

15 (*a*) Z. Li, N. Cai, Y. Huang and H. Han, *Energy Fuels*, 2005, **19**, 1447–1452; (*b*) Z. Li, N. Cai and Y. Huang, *Ind. Eng. Chem. Res.*, 2006, **45**, 1911–1917; (*c*) C. S. Martavaltzi and A. A. Lemonidou, *Microporous Mesoporous Mater.*, 2008, **110**, 119–127; (*d*) C. S. Martavaltzi and A. A. Lemonidou, *Ind. Eng. Chem. Res.*, 2008, **47**, 9537–9543.

16 Z. Yang, M. Zhao, N. H. Florin and A. T. Harris, *Ind. Eng. Chem. Res.*, 2009, **123**, 10765–10770.

17 (*a*) J. Blamey, N. P. M. Paterson, D. R. Dugwell and P. S. Fennell, *Energy Fuels*, 2010, **24**, 4605–4616; (*b*) V. Manovic and E. J. Anthony, *Fuel*, 2011, **90**, 233–239; (*c*) K. Kuramoto, S. Fujimoto, A. Morita, S. Shibano, Y. Suzuki, H. Hatano, L. Shi-Ying, M. Harada and T. Takarada, *Ind. Eng. Chem. Res.*, 2003, **42**, 975–981.

18 (*a*) G. L. Messing, S.-C. Zhang and G. V. Jayanthi, *J. Am. Ceram. Soc.*, 1993, **76**, 2707–2726; (*b*) A. B. D. Nandiyanto and K. Okuyama, *Adv. Powder Technol.*, 2011, **22**, 1–19; (*c*) J. H. Bang and K. S. Suslick, *Adv. Mater.*, 2010, **22**, 1039–1059.

19 (*a*) J. H. Bang, Y. T. Didenko, R. J. Helmich and K. S. Suslick, *Aldrich Material Matters*, 2012, **7**, 15–20; (*b*) T. T. Kodas and M. J. Hampden-Smith, *Aerosol Processing of Materials*, Wiley-VCH, New York, 1999.

20 (*a*) W. H. Suh, A. R. Jang, Y.-H. Suh and K. S. Suslick, *Adv. Mater.*, 2006, **18**, 1832–1837; (*b*) R. J. Helmich and K. S. Suslick, *Chem. Mater.*, 2010, **22**, 4835–4837.